J Mol Model (2013) 19:3325–3332
DOI 10.1007/s00894-013-1863-3

ORIGINAL PAPER

Relativistic theoretical studies on hydrogen bonds and the electronic structure of aqueous solvated *bis*(uranyl) complex: an insight into explicit and/or implicit solvent effects

Yuan-Ru Guo · Xin Zhou · Qing-Jiang Pan

Received: 2 March 2013 / Accepted: 18 April 2013 / Published online: 12 May 2013

Abstract To understand the chemical behavior of uranyl complexes in water, a bis-uranyl $[(phen)(UO_2)(\mu_2\text{–}F)(F)]_2$ (**A**; phen=phenanthroline, μ_2=doubly bridged) and its hydrated form $\mathbf{A}\cdot(H_2O)_n$ (n=2, 4 and 6) were examined using scalar relativistic density functional theory. The addition of water caused the phen ligands to deviate slightly from the $U_2(\mu_2\text{–}F)_2$ plane, and red-shifts the U–F-terminal and U=O stretching vibrations. Four types of hydrogen bonds are present in the optimized hydrated $\mathbf{A}\cdot(H_2O)_n$ complexes; their energies were calculated to fall within the range 4.37–6.77 kcal mol^{-1}, comparable to the typical values of 5.0 kcal mol^{-1} reported for hydrogen bonds. An aqueous environment simulated by explicit and/or implicit models lowers and re-arranges the orbitals of the bis-uranyl complex.

Keywords Bis-uranyl complex · Hydrogen bond · Electronic structure · Solvent effect · Relativistic DFT

Electronic supplementary material The online version of this article (doi:10.1007/s00894-013-1863-3) contains supplementary material, which is available to authorized users.

Y.-R. Guo
Key Laboratory of Bio-based Material Science and Technology of Education Ministry, College of Material Science and Engineering, Northeast Forestry University, Harbin 150040, China

Q.-J. Pan (✉)
Key Laboratory of Functional Inorganic Material Chemistry of Education Ministry, School of Chemistry and Materials Science, Heilongjiang University, Harbin 150080, China
e-mail: panqjitc@163.com

X. Zhou
Institute of Theoretical and Simulation Chemistry, Academy of Fundamental and Interdisciplinary Science, Harbin Institute of Technology, Harbin 150008, China

Introduction

The early 5f-element uranium has interesting electronic and structural properties due to the accessibility of its rich *s*, *p*, *d* and *f* orbitals for chemical bonding [1, 2]. It reacts with a variety of organic and inorganic ligands and displays oxidation states from III to VI. In most processing and environmental conditions, the hexavalent UO_2^{2+} ion is the most prevalent and most thermodynamically stable form of uranium. This ion is highly soluble and mobile, and eventually biologically available, causing long-term environmental risks [3, 4]. Additionally, uranyl ion has been extensively studied for over half a century because of its utmost importance in the processing of nuclear fuel and the disposal of nuclear waste [3].

Due to the strongly covalent nature of axial U=O bonds, the uranyl ion is extraordinarily chemically robust [5]. This makes uranyl coordination chemistry much more active in the equatorial plane [2, 5–7], although its axial chemistry has been developed recently via uranyl oxo functionalization [8, 9] and cation–cation interactions (uranyl interaction with actinyl and metal ions) [10–12]. In general, the uranyl ion is equatorially coordinated by four to six ligands [2, 5]. These ligands are diverse and include halide, THF, pyridine, polypyridine, pyrrole and polypyrrole (porphyrin, expanded porphyrin and calixpyrroles) [7, 13–16]. In this respect, we have recently synthesized a bis(uranyl) complex, labeled **A** in this paper (see Chart 1): $[(phen)(UO_2)(\mu_2\text{–}F)(F)]_2$ (phen= phenanthroline, μ_2=doubly bridged) using the solvothermal method [17]. Single crystal X-ray diffraction revealed its dimeric structure with edge-sharing pentagonal bipyramids, where F^- ions serve as both terminal and bridging ligands to link uranium centers. In the synthesis, hydrofluoric acid was used as a major F^- source, which has implications for the mineralization and crystallization of uranyl complexes. Due

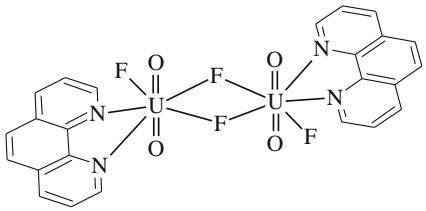

Chart 1 Structure of $[(phen)(UO_2)(\mu_2–F)(F)]_2$ (**A**)

to its simple molecular structure and good solubility in water, complex **A** is a good candidate with which to study the electronic structures and aqueous coordination chemistry of uranyl species.

With the goal of developing actinyl coordination chemistry and providing support for the nuclear processing and purification strategies, it is essential to explore the structural and electronic properties of complexes in the aqueous solution. In this work, we used relativistic density functional theory (DFT) to study the bis(actinyl) complex **A** and its aqueous solvated species. The effects of hydrogen bonds on geometry and vibrational spectra were addressed. Explicit and/or implicit solvent environments were taken into account for accurate electronic structure calculations.

Computational details

Our newly synthesized bis(uranyl) complex, $[(phen)(U^{VI}O_2)(\mu_2–F)(F)]_2$ (**A**), was investigated theoretically in this work. To consider the aqueous environment, three solvent models were used. The first is an explicit solvent model, simulated by **A** $(H_2O)_n$ (labeled as **A** nW; n=2, 4 and 6), where water molecules are placed around **A** and the hydrogen bonds formed can stabilize the whole molecular system. The second is an implicit model, where aqueous continuum dielectric (described below) was taken into account in the calculations of **A**, denoted by **A**(sol). Third, both explicit and implicit solvation were included when calculating **A** nW with the aqueous continuum dielectric model. We used **A** nW(sol) to stand for this case. And thus, **A**, **A** nW, **A**(sol) and **A** nW(sol) represent calculations in the gas phase, the explicit aqueous solution, the implicit aqueous solution, and the explicit and implicit aqueous solution, respectively.

All structural optimizations of **A** and **A** nW (n=2, 4 and 6) were accomplished with the Priroda code [18–20]. Relativistic DFT with the Perdew, Burke and Ernzerhof (PBE) functional [21] was applied in these calculations. All-electron correlation-consistent double-ς polarized quality Gaussian basis sets (labeled as L1 in the text) were used for the large component, accompanied by the corresponding kinetically balanced basis sets for the small component [19]. A scalar relativistic all-electron (AE) approach [20] is applied in Priroda, which makes use of the full Dirac equation but with spin-orbit projected out and neglected [22]. We performed frequency calculations to confirm that the obtainable structures are minimum points on the potential energy surface. Simultaneously, thermodynamic data and vibrational spectra of the complexes were obtained. Population-based Mayer [23] bond orders were calculated based on these PBE calculations.

At the Priroda-optimized geometry, single-point calculations were performed using the ADF 2010.02 code [24–26] to obtain electronic structure in gas phase and in solution. The implicit solvent effects of water were taken into account by the COSMO model [27] as implemented in ADF. An integration parameter of 6.0 was applied. Klamt radii were used for atoms of U=1.70 Å, H=1.30 Å, C=2.00 Å, N=1.83 Å, O=1.72 Å and F=1.76 Å [28–31]. So we applied the PBE functional, triple-ς polarized quality (TZP) basis sets and the scalar relativistic ZORA approach in the calculations.

Results and discussion

Geometry structures

The optimized structures of **A** and **A** nW (n=2, 4 and 6) at the PBE/L1/AE level are presented in Fig. 1. Selected geometry parameters and bond orders are listed in Table 1. As seen in the figure, the parent complex **A** was calculated to display a dimeric structure formed by edge-sharing pentagonal bipyramids. This is consistent with the experimentally reported structure from single crystal X-ray diffraction [17]. All the calculated dihedral angles of U1-F1-F2-U2, N2-U1-F1-F2 and F3-U1-F2-F1 are 180° (Table 1), indicating that the phenanthroline and fluorine ligands are located in the equatorial plane of the uranyl cations. The two linear uranyl cations are nearly parallel and approximately perpendicular to the plane. Calculations on **A** nW (n=2, 4 and 6) demonstrate that the addition of water has no effect on the $U_2(\mu_2–F)_2$-core plane, which still retains the 180° U1-F1-F2-U2 angle. The terminal-F has a very small distortion, reflected by 177°–180° F3-U1-F2-F1 angles. In contrast, the phenanthroline ligands deviate slightly from the $U_2(\mu_2–F)_2$-core plane, with the largest deviation of 11° seen for the solvated **A** 4W (Table 1).

Compared with **A**, the introduction of water into **A** nW lengthens the U=O and U–F-terminal bonds. The calculated elongation is less than 0.03 Å. The explicit aqueous solvation indirectly shortens almost all the U–F-bridging and U–N bonds of **A** nW. Interaction of the hydrogen atoms of water with the uranyl oxygen and terminal-fluorine of **A** generates hydrogen bonds, weakening the U=O and U–F-terminal bonds. Consequently, more electrons from the uranium center originally involved in the U=O and U–F-terminal bonds is released, strengthening the equatorial U–F-bridging and U–N bonds.

As shown in Table 1, the calculated U=O bond orders range from 2.30 to 2.37 for **A** and **A** nW (n=2, 4 and 6),

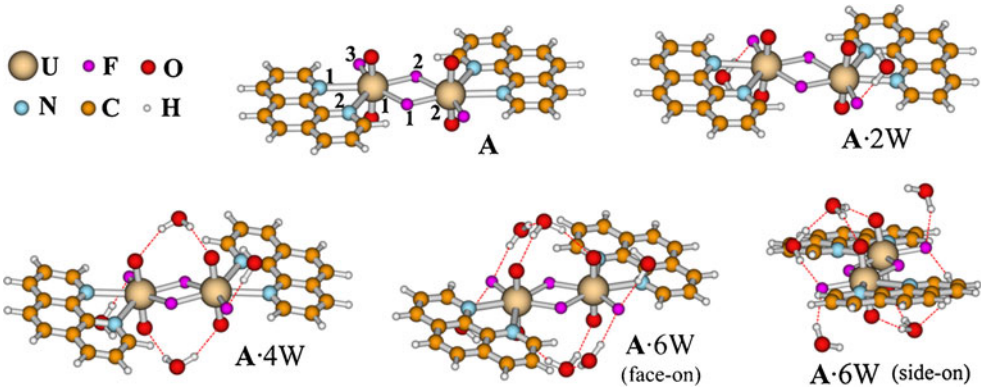

Fig. 1 Optimized structures of the parent complex $[(phen)(UO_2)(\mu_2\text{–}F)(F)]_2$ (**A**) and its solvated form $\mathbf{A}\cdot(H_2O)_n$ (**A** nW; n=2, 4 and 6). A 6W is depicted in face-on view and side-on view to show hydrogen bonds clearly

suggesting a partial triple bond character. Upon increasing the explicit water, the U=O bond orders decrease in sequence. In the equatorial plane, one strong single U–F-terminal bond is formed, and four relatively weak single bonds include two bridging-F→U and two N→U.

Hydrogen bonds

Four types of hydrogen bonds, H···F-*terminal*, H···O_{yl} (uranyl oxo), H···O_w (water oxo) and H_{phen}···O_w (phen hydrogen), are present in the hydrated **A** nW (n=2, 4 and 6). The calculated distances are given in Table 2, associated with the number of each type of hydrogen bond in **A** nW. The shortest hydrogen bond, which is formed between water molecules (H···O_w) in **A** 6W, was calculated to be 1.84 Å. The calculated H···F-terminal distances fall within 1.91 and 2.10 Å. As the majority of valence electrons of uranyl oxygen are involved in the U=O bonding, its weak basicity leads to relatively long H···O_{yl} bond lengths ranging from 1.99 to 2.42 Å. We also calculated the H_{phen}···O_w bond at 2.06 Å in **A** 6W, showing weaker bonding strength than H···O_w but being similar to H···O_{yl}.

Given that hydrogen bonds occur in **A** nW (n=2, 4 and 6), their hydrated energies (ΔE) can be calculated as follows:

$$\Delta E = E(A) + nE(H_2O) - E(\mathbf{A}\cdot nW) \quad (1)$$

where E(**A**), E(H_2O) and E(**A** nW) correspond to total energies of **A**, H_2O and **A** nW at their respective optimized geometries. According to Eq. (1), greater ΔE denotes stronger hydrogen bonds. As shown in Table 2, the ΔE of **A** nW (n=2, 4 and 6) were calculated to be 19.54, 39.59 and 73.18 kcal mol^{-1}, respectively.

Regarding the H···F-terminal, H···O_{yl}, H···O_w and H_{phen}···O_w hydrogen bonds, each type has some common nature. This allows us to assume that the energy of each type of hydrogen bond [E(type)] is approximately inversely proportional to its bond length (r in angstrom), see Eq. (2).

Table 1 Optimized geometry parameters and bond orders (in parentheses) for $[(phen)(UO_2)(\mu_2\text{–}F)(F)]_2$ (**A**) and its solvated form $\mathbf{A}\cdot(H_2O)_n$ (**A** nW; n=2, 4 and 6), compared with experimental values from single crystal X-ray diffraction (distances in Ångstroms and angles in degrees)

	A [a]		**A**·2W	**A**·4W	**A**·6W
	Calculated	Experimental	Calculated	Calculated	Calculated
U1=O	1.808 (2.37)	1.781	1.808 (2.34)	1.818 (2.31)	1.818 (2.30)
U1-F1	2.363 (0.54)	2.353	2.351 (0.55)	2.351 (0.56)	2.335 (0.55)
U1-F2	2.329 (0.55)	2.334	2.329 (0.55)	2.305 (0.59)	2.311 (0.60)
U1-F3	2.126 (1.13)	2.132	2.150 (1.05)	2.137 (1.09)	2.157 (1.03)
U1-N1	2.650 (0.31)	2.588	2.633 (0.32)	2.628 (0.33)	2.604 (0.35)
U1-N2	2.684 (0.31)	2.626	2.668 (0.32)	2.652 (0.34)	2.634 (0.36)
U1···U2	3.911 (0.06)	3.929	3.907 (0.06)	3.883 (0.06)	3.890 (0.07)
O=U=O	172.6	175.2	173.3	176.8	174.4
O-U1-U2	91.7	90.7	91.8	90.4	91.1
F1-U1-F2	67.1	66.1	66.8	67.0	66.3
U1-F1-U2	112.9	113.9	113.2	113.0	113.7
U1-F1-F2-U2	180.0	180.0	180.0	180.0	180.0
N2-U1-F1-F2	180.0	179.9	178.9	169.1	174.3
F3-U1-F2-F1	180.0	180.0	179.7	176.6	176.8

[a]Experimental and calculated values from [17]

Table 2 Calculated energies (kcal mol^{-1}) of hydration and hydrogen bond of **A**, associated with the number of each type of hydrogen bond

	A·2W	**A**·4W	**A**·6W
Hydration energy (kcal mol^{-1}) of **A**			
$\Delta E/\Delta E_0$ [a]	19.54/15.53	39.59/31.08	73.18/59.12
Energy (kcal mol^{-1}) and distance (Å) of hydrogen bond			
$(H\cdots F)_1$ [b]	5.25 [c]/4.26 [d] (1.912) [e]	5.18/4.20 (1.939)	5.13/4.16 (1.959)
$(H\cdots F)_2$ [b]	–	–	4.79/3.88 (2.097)
$(H\cdots O_{yl})_1$	4.52/3.50 (2.343)	4.44/3.44 (2.385)	4.37/3.39 (2.421)
$(H\cdots O_{yl})_2$	–	5.10/3.95 (2.077)	5.07/3.93 (2.087)
$(H\cdots O_{yl})_3$	–	5.08/3.94 (2.083)	5.32/4.13 (1.990)
$(H\cdots O_w)$	–	–	6.77/6.07 (1.839)
$(H_{phen}\cdots O_w)$	–	–	5.14/3.99 (2.058)
Number of hydrogen bonds			
N(H···F) [b]	2	2	4
$N(H\cdots O_{yl})$	2	6	6
$N(H\cdots O_w)$	–	–	2
$N(H_{phen}\cdots O_w)$	–	–	2

[a] ΔE and ΔE_0 denote the total energy excluding and including zero-point vibration energy (ZPVE) in the hydrated process of **A**, respectively

[b] The fluorine atom is the terminal one

[c] Calculated energy of hydrogen bond (E(type)) from ΔE

[d] Calculated energy of hydrogen bond (E(type)) from ΔE_0

[e] Optimized distance of hydrogen bond in Å

Thus each type of hydrogen bond has an identical proportional coefficient c(type). Associated with the number of each type of hydrogen bond [N(type)], we are able to construct Eq. (3):

$$E(\text{type}) = \frac{c(\text{type})}{r} \tag{2}$$

$$\sum_{\text{type}} N(\text{type})E(\text{type}) = \sum_{\text{type}} \frac{N(\text{type})c(\text{type})}{r} = \Delta E \tag{3}$$

According to Table 2, three equations with four c(type) parameters were built. We further assume that the $H_{phen}\cdots O_w$ and $H\cdots O_{yl}$ bonds have approximately identical c(type) values, i.e., showing identical bonding strength in unit distance.

Finally, the energy of each hydrogen bond was calculated (listed in Table 2). The $H\cdots O_w$ bond has the largest energy of 6.77 kcal mol^{-1}, whereas the smallest energy of 4.37 kcal mol^{-1} belongs to the $H\cdots O_{yl}$ bond. These values correspond to hydrogen bond distances of 1.84 and 2.42 Å, respectively. The calculated energies of hydrogen bonds involved in **A** nW (n=2, 4 and 6) all agree well with the reported typical 5.0 kcal mol^{-1} energy of hydrogen bonds in water [32]. When further considering the zero-point vibration energy (ZPVE), frequency calculations gave total energy containing ZPVE (ΔE_0) at 15.53, 31.08 and 59.12 kcal mol^{-1} for **A** nW (n=2, 4 and 6), respectively (Table 2). Using the same equation and approximation, their bonding energies were calculated to be within 3.39 and 6.07 kcal mol^{-1}.

Vibrational spectra

Building on frequency calculations, vibrational spectra of **A** and **A** nW (n=2, 4 and 6) were simulated in Fig. 2 using Lorentzian broadening. **A** and **A** nW (n=2, 4 and 6) can be seen to have a similar general pattern of vibrational spectra. Moreover, these theoretically simulated spectra are comparable to experimentally measured infrared (IR) spectra [17].

With respect to **A**, two strong bands calculated at 824 and 906 cm^{-1} were assigned to the U=O symmetric and asymmetric stretching modes, respectively. They remain unchanged in **A** 2W, but are red-shifted to 801 and 885 cm^{-1} in **A** 4W and **A** 6W. This is related to the weakening of U=O bonds due to the interaction of additional hydrogen bonds. Note that the calculated wave numbers of characteristic U=O vibration bands are lower than the experimental values of 850 and 916 cm^{-1}. The GGA functionals is known to slightly underestimate bond strengths and corresponding stretching frequencies [17, 29–31]. On the other hand, the experimental IR spectra were measured in the solid state, while only gas-phase or solvated complexes were considered in the calculations. These different molecular environments may be one of the factors generating the discrepancy.

Compared with the vibrational modes of **A**, stretching vibration of the terminal-F–U bond in **A** nW (n=2, 4 and 6) is found in the lower-energy region. The explicit aqueous solvation weakens the bonding strength and leads to a large red-shift of 25–40 cm^{-1}. The bridging-F–U vibration of **A** nW (n=2, 4 and 6) was calculated to be 370 cm^{-1} (mean value), close to 374 cm^{-1} of **A**. It is further evident that no bridging-F atom participates in the hydrogen bonds mentioned above. Additionally, the theoretical 717 cm^{-1} of **A**

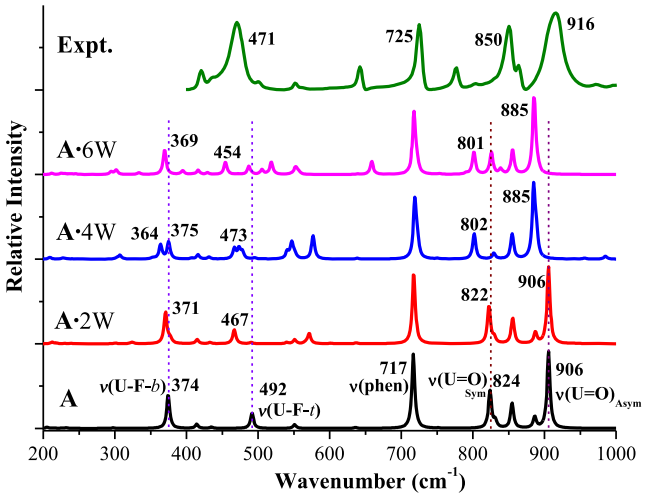

Fig. 2 Simulated vibrational spectra of bis-uranyl **A** and its solvated form **A** nW (n=2, 4 and 6), together with experimental infrared (IR) measurements

and **A** nW corresponds to the experimental peak at 725 cm^{-1}, being characteristic of phenanthroline.

Electronic structures

In this work, the electronic structures of **A** and **A** nW (n=2, 4 and 6) were calculated at the PBE/TZP/ZORA level while excluding and including the COSMO solvent model. Energy levels of frontier molecular orbitals of **A** in the gas-phase and aqueous environments are presented in Figure S1 of the Supplementary Material. The corresponding values of HOMO and LUMO as well as their gaps are given in Table 3. In the gas phase, the HOMO/LUMO energies of **A** were calculated to be −5.86/−3.21 eV with a 2.64 eV energy gap. By comparison, the addition of explicit water stabilizes the overall orbitals of **A** nW (n=2, 4 and 6). The lowering of HOMOs of **A** nW greater than LUMOs permits narrowing of all the HOMO–LUMO gaps. Moreover, these H–L gaps decrease in sequence upon increasing the number of explicit water molecules. A similar case is found in **A**(sol) and **A** nW(sol) while including the implicit COSMO solvation. For example, **A**(sol) presents a smaller gap of 2.09 eV than the 2.64 eV of **A**.

To provide an insight into the structural properties and chemical behaviors of uranyl complexes, detailed compositions of the frontier orbitals of **A**, **A** nW, **A**(sol) and **A** nW(sol) (n=2, 4 and 6) are presented in Table 4, Table S1 and Table S2. Building on these results, unoccupied orbitals of all the complexes are featured with U(f) character. Explicit and/or implicit aqueous solvation does not change their order and character, albeit their energies are lowered.

However, the order and character of occupied orbitals are sensitive to the choice of solvent model. As shown in Table 4, HOMO and H-1 of **A** in the gas phase are contributed by σ(U=O) bonding, followed by four lower-energy phen-based orbitals. With respect to **A**(sol), implicit solvation raises the phen-based orbitals to form HOMO–H-4, while energies of σ(U=O) bonding orbitals are lowered ,yielding H-4 and H-5. Regarding **A** 2W, the explicit model introduces the contribution of water, constituting HOMO and H-1. Simultaneously, orbitals with σ(U=O) and phen combined character are present. When considering **A** 2W(sol), the basic order of orbitals of **A**(sol) is retained, but with H_2O orbitals inserted between orbitals of higher-energy phen and lower-energy σ(U=O). In Fig. 3, we have depicted intuitively the energy levels of orbitals, character and electron-density diagrams for the complexes discussed above. Explicit and/or implicit solvation was found to rearrange occupied orbitals, and lower their energies, especially for σ(U=O) orbitals.

Finally, let us focus on the characteristic orbitals of **A** nW and **A** nW(sol) (n=0, 2, 4 and 6) such as occupied orbitals with the character of σ(U=O), π(phen) and H_2O as well as LUMO with U(f_{z^2y},$f_{y(3x^2-y^2)}$). As more than one filled orbital has σ(U=O), π(phen) and H_2O composition, we will address only the highest-energy one. Energy differences between each characteristic occupied orbital and LUMO (Table 3) represent possible electronic excitation transitions, providing an implication for the absorption and emission of the complex. In the gas phase, **A** displays a σ(U=O)→U(f) (LUMO) transition at 2.64 eV and π(phen)→U(f) at 3.18 eV. The featured transition of H_2O→U(f) becomes lowest-energy in **A** nW (n=2, 4 and 6). Upon introducing implicit solvation into **A** and **A** nW (n=2, 4 and 6), the π(phen)→U(f) transition turns out to be the lowest-energy one. It is worth noting that all the σ(U=O)→U(f)

Table 3 Energies (eV) of HOMO, LUMO and their gaps in **A** nW and **A** nW(sol) (n=0, 2, 4 and 6), together with energies of transition from characteristic orbitals [σ(U=O), π(phen) and H_2O] to LUMO [U(f_{z^2y}, $f_{y(3x^2-y^2)}$)]

	A	**A**·2W	**A**·4W	**A**·6W	**A**(sol)	**A**·2W(sol)	**A**·4W(sol)	**A**·6W(sol)
HOMO	−5.86	−5.94	−6.08	−6.06	−6.38	−6.38	−6.38	−6.41
LUMO	−3.21	−3.67	−4.07	−4.34	−4.30	−4.44	−4.60	−4.71
H-L Gap	2.64	2.27	2.00	1.71	2.09	1.94	1.78	1.70
σ(U=O)→U(f)	2.64	2.67	2.68	2.70	2.73	2.74	2.66	2.71
π(phen)→U(f)	3.18	3.19	2.47	2.32	2.09	1.94	1.78	1.70
H_2O→U(f)	–	2.27	2.00	1.71	–	2.56	2.42	2.35

Table 4 Calculated partial molecular orbital contributions (%) and orbital energy (eV) of **A**, **A**(sol), **A** 2W and **A** 2W(sol)

	A		**A**(sol)		**A**·2W		**A**·2W(sol)	
Orbitals	Energy	Composition	Energy	Composition	Energy	Composition	Energy	Composition
L+5	−3.054	91 % U(f_{z^3}, $f_{z(x^2-y^2)}$, $f_z{}^2{}_x$)	−4.053	93 % U(f_{xyz}, $f_z{}^2{}_y$, $f_{y(3x^2-y^2)}$)	−3.457	88 % U(f_{xyz}, $f_z{}^2{}_y$, $f_{y(3x^2-y^2)}$)	−4.220	96 % U(f_{xyz}, $f_z{}^2{}_y$, $f_{y(3x^2-y^2)}$)
L+4	−3.089	75 % phen, 15 % U(f_{xyz})	−4.100	89 % U(f_{z^3}, $f_{z(x^2-y^2)}$, $f_z{}^2{}_x$)	−3.524	91 % U(f_{z^3}, $f_{z(x^2-y^2)}$, $f_z{}^2{}_x$)	−4.258	90 % U(f_{z^3}, $f_{z(x^2-y^2)}$, $f_z{}^2{}_x$)
L+3	−3.128	55 % U(f_{xyz}), 38 % phen	−4.172	94 % U(f_{xyz})	−3.572	90 % U(f_{xyz})	−4.339	94 % U(f_{xyz})
L+2	−3.148	87 % U($f_z{}^2{}_y$, $f_{y(3x^2-y^2)}$, f_{xyz})	−4.221	97 % U($f_z{}^2{}_y$, $f_{y(3x^2-y^2)}$, f_{xyz})	−3.600	95 % U($f_z{}^2{}_y$, $f_{y(3x^2-y^2)}$, f_{xyz})	−4.365	95 % U($f_z{}^2{}_y$, $f_{y(3x^2-y^2)}$, f_{xyz})
L+1	−3.195	93 % U(f_{z^3}, $f_{z(x^2-y^2)}$, $f_z{}^2{}_x$)	−4.239	93 % U(f_{z^3}, $f_{z(x^2-y^2)}$, $f_z{}^2{}_x$)	−3.661	91 % U(f_{z^3}, $f_{z(x^2-y^2)}$, $f_z{}^2{}_x$)	−4.392	89 % U(f_{z^3}, $f_{z(x^2-y^2)}$, $f_z{}^2{}_x$)
LUMO	−3.214	92 % U($f_z{}^2{}_y$, $f_{y(3x^2-y^2)}$)	−4.297	97 % U($f_z{}^2{}_y$, $f_{y(3x^2-y^2)}$)	−3.674	96 % U($f_z{}^2{}_y$, $f_{y(3x^2-y^2)}$)	−4.444	98 % U($f_z{}^2{}_y$, $f_{y(3x^2-y^2)}$)
HOMO	−5.857	45 % U($f_{y(3x^2-y^2)}$, $f_z{}^2{}_y$, p_y), 35 % O(p_y), 16 % F(p_y)	−6.384	90 % phen	−5.943	91 % H_2O	−6.380	89 % phen
H-1	−6.000	45 % U($f_{y(3x^2-y^2)}$, p_y, $f_z{}^2{}_y$), 35 % O(p_y), 12 % F(p_y)	−6.384	90 % phen	−5.944	91 % H_2O	−6.381	89 % phen
H-2	−6.395	92 % phen	−6.766	92 % phen	−6.346	44 % U($f_{y(3x^2-y^2)}$, $f_z{}^2{}_y$, p_y), 34 % O(p_y), 14 % F(p_y)	−6.759	88 % phen
H-3	−6.403	91 % phen	−6.767	92 % phen	−6.468	38 % phen, 27 % U($f_{y(3x^2-y^2)}$, $f_z{}^2{}_y$, p_y), 20 % O(p_y), 4 % F(p_y)	−6.759	82 % phen
H-4	−6.740	88 % phen	−7.026	44 % U($f_{y(3x^2-y^2)}$, $f_z{}^2{}_y$), 35 % O($2p_y$), 17 % F(p_y)	−6.536	85 % phen	−7.004	87 % H_2O
H-5	−6.745	89 % phen	−7.183	45 % U($f_{y(3x^2-y^2)}$, $f_z{}^2{}_y$), 35 % O($2p_y$), 13 % F(p_y)	−6.589	45 % phen, 21 % U($f_{y(3x^2-y^2)}$, $f_z{}^2{}_y$, p_y), 16 % O(p_y), 7 % F(p_y)	−7.005	85 % H_2O
H-6					−6.859	91 % phen	−7.188	45 % U($f_{y(3x^2-y^2)}$, $f_z{}^2{}_y$, p_y), 35 % O(p_y), 15 % F(p_y)
H-7					−6.861	91 % phen	−7.363	47 % U($f_{y(3x^2-y^2)}$, $f_z{}^2{}_y$, p_y), 35 % O(p_y), 11 % F(p_y)

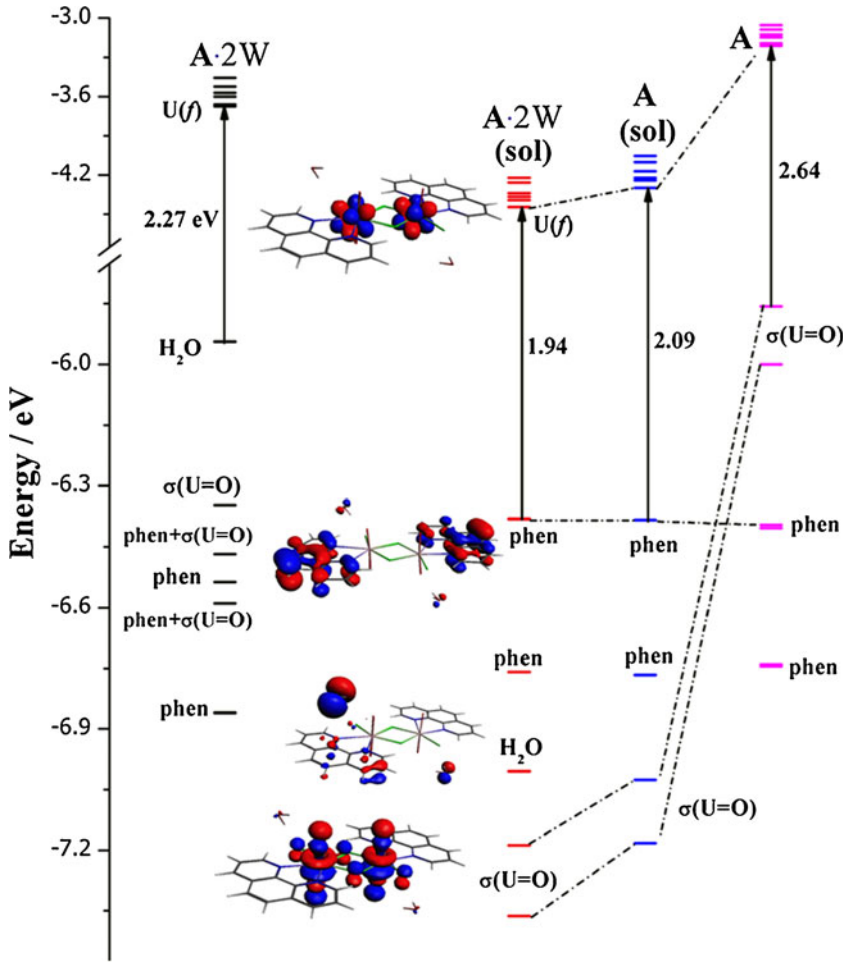

Fig. 3 Energy levels of frontier molecular orbitals and electron density diagrams of typical U(*f*), π(phen), σ(U=O) and H_2O orbitals for **A**, **A** 2W, **A**(sol) and **A** 2W(sol)

transition of **A**, whether in the gas phase or in solution, has energy close to within 2.64–2.74 eV (in Table 3). This reveals that the σ(U=O)→U(*f*) transitions (absorption and emission) are intrinsic to the uranyl complex. These featured transitions are independent of its environment (gas phase, solution and even solid state).

Conclusions

In the work, the bis-uranyl complex **A** and its solvated form **A** nW (n=2, 4 and 6) were examined using scalar relativistic DFT. The hydrogen bonds generated and their relationship with vibrational spectra, geometrical and electronic structures were explored. The following conclusions have been drawn:

Full optimizations demonstrate that the addition of water causes phen ligands to deviate slightly from the $U_2(\mu_2\text{-}F)_2$ core plane. The generated hydrogen bonds lengthen the U=O and U-F-terminal distances. As a result, partial valance electron of the uranium center originally involved in such bonds is released. This eventually shortens the U–F-bridging e and U–N bond lengths. Compared with those of **A**, the U–F-terminal and U=O stretching vibrations of **A**·nW (n=2, 4 and 6) are red-shifted by hydrogen bonds. It is also evidenced by the elongation of U–F-terminal and U=O bonds. Because there is no direct hydrogen bonding interaction with bridging-F atoms, a negligible spectral shift is found for U–F-bridging vibrations.

Building on their type, bond length and number, energies of hydrogen bonds (H···F, H···O_{yl}, H···O_w and H_{phen}···O_w) were calculated to fall within 4.37–6.77 kcal mol^{-1}. These results agree well with typical values of reported hydrogen bonds. When including ZPVE, smaller bonding energies ranging from 3.39 to 6.07 kcal mol^{-1} were obtained.

Finally, the effects of explicit and/or implicit aqueous environment on the electronic structures of **A** were investigated. It was shown that solvation should be taken into account for accurate electronic structure calculations. Compared with those of **A** in the gas phase, aqueous solvation lowers energy levels of orbitals and re-orders molecular orbitals. The present study also reveals that the bis-uranyl **A** has an intrinsic σ(U=O)→U(*f*) transition, whose excitation energy is insensitive to molecular environment.

Acknowledgments Q.J.P. is grateful to Dr. Dimitri Laikov for providing the Priroda code. This work is supported by Fundamental Research Funds for the Central Universities (DL11CB07), National Natural Science Foundation of China (21273063), Program for New Century Excellent Talents in University (NCET-11-0958), Key Project of Chinese Ministry of Education (211048), and Program for Innovative Research Team in University (IRT-1237). Foundations of Heilongjiang Province (LC2011C22, 1154-NCET-010) and of State Education Ministry for the Returned Overseas Chinese Scholars are greatly acknowledged.

References

1. Kaltsoyannis N, Scott P (1999) The f elements. Oxford Science, Oxford, UK
2. Bart SC, Meyer K (2008) Organometallic and coordination chemistry of the actinides. Springer, Berlin, p 119
3. Hashke JM, Stakebake JL (2006) In: Morss LR, Edelstein NM, Fuger J (eds) The chemistry of the actinide and transactinide elements. Springer, Berlin, p 3199
4. Choppin GR (2007) J Radioanal Nucl Chem 273:695
5. Denning RG (2007) J Phys Chem A 111:4125
6. Berthet JC, Nierlich M, Ephritikhine M (2003) Angew Chem Int Ed 42:1952
7. Vaughn AE, Barnes CL, Duval PB (2007) J Chem Crystallogr 37:779
8. Fortier S, Hayton TW (2010) Coord Chem Rev 254:197
9. Hayton TW (2010) Dalton Trans 39:1145
10. Nocton G, Horeglad P, Pecaut J, Mazzanti M (2008) J Am Chem Soc 130:16633
11. Sullens TA, Jensen RA, Shvareva TY, Albrecht-Schmitt TE (2004) J Am Chem Soc 126:2676
12. Arnold PL, Jones GM, Odoh SO, Schreckenbach G, Magnani N, Love JB (2012) Nat Chem 4:221
13. Oldham WJ, Oldham SM, Scott BL, Abney KD, Smith WH, Costa DA (2001) Chem Commun 1348
14. Sessler JL, Melfi PJ, Pantos GD (2006) Coord Chem Rev 250:816
15. Love JB (2009) Chem Commun 3154
16. Natrajan L, Burdet F, Pecaut J, Mazzanti M (2006) J Am Chem Soc 128:7152
17. Pan Q-J, Wang Y-M, Wang R-X, Wu H-Y, Yang W, Sun Z-M, Zhang H-X (2013) RSC Adv 3:1572
18. Laikov DN (2007) J Comput Chem 28:698
19. Laikov DN (2005) Chem Phys Lett 416:116
20. Laikov DN (2000) An implementation of the scalar relativistic density functional theory for molecular calculatios with Gaussian basis sets, DFT2000 Conference, Menton, France
21. Perdew JP, Burke K, Ernzerhof M (1996) Phys Rev Lett 77:3865
22. Dyall KG (1994) J Chem Phys 100:2118
23. Mayer I (2003) Simple theorems, proof and derivations in quantum chemistry. Kluwer/Plenum, New York
24. Velde GT, Bickelhaupt FM, Baerends EJ, Guerra CF, Van Gisbergen SJA, Snijders JG, Ziegler T (2001) J Comput Chem 22:931
25. Guerra CF, Snijders JG, te Velde G, Baerends EJ (1998) Theor Chem Acc 99:391
26. Baerends EJ, Ziegler T, Autschbach J, Bashford D, Bérces A, Bickelhaupt FM, Bo C, Boerrigter PM, Cavallo L, Chong DP, Deng L, Dickson RM, Ellis DE, van Faassen M, Fan L, Fischer TH, Fonseca Guerra C, Ghysels A, Giammona A, van Gisbergen SJA, Götz AW, Groeneveld JA, Gritsenko OV, Grüning M, Gusarov S, Harris FE, van den Hoek P, Jacob CR, Jacobsen H, Jensen L, Kaminski JW, van Kessel G, Kootstra F, Kovalenko A, Krykunov MV, van Lenthe E, McCormack DA, Michalak A, Mitoraj M, Neugebauer J, Nicu VP, Noodleman L, Osinga VP, Patchkovskii S, Philipsen PHT, Post D, Pye CC, Ravenek W, Rodríguez JI, Ros P, Schipper PRT, Schreckenbach G, Seldenthuis JS, Seth M, Snijders JG, Solà M, Swart M, Swerhone D, te Velde G, Vernooijs P, Versluis L, Visscher L, Visser O, Wang F, Wesolowski TA, van Wezenbeek EM, Wiesenekker G, Wolff SK, Woo TK, Yakovlev AL (2010) ADF. SCM, Theoretical Chemistry, Vrije Universiteit, Amsterdam
27. Pye CC, Ziegler T (1999) Theor Chem Acc 101:396
28. Klamt A, Jonas V, Burger T, Lohrenz JCW (1998) J Phys Chem A 102:5074
29. Shamov GA (2011) J Am Chem Soc 133:4316
30. Pan Q-J, Schreckenbach G, Arnold PL, Love JB (2011) Chem Commun 47:5720
31. Pan QJ, Shamov GA, Schreckenbach G (2010) Chem Eur J 16:2282
32. From Wikipedia, the free encyclopedia. http://en.wikipedia.org/wiki/Hydrogen_bond